Mechanistic Rationale to Target PTEN-Deficient Tumor Cells with Inhibitors of the DNA Damage Response Kinase ATM

McCabe, N., Hanna, C., Walker, S. M., Gonda, D., Li, J., Wikstrom, K., ... Kennedy, R. D. (2015). Mechanistic Rationale to Target PTEN-Deficient Tumor Cells with Inhibitors of the DNA Damage Response Kinase ATM. Cancer Research, 75(11), 2159-2165. DOI: 10.1158/0008-5472.CAN-14-3502

Published in:
Cancer Research

Document Version:
Peer reviewed version

Queen's University Belfast - Research Portal:
Link to publication record in Queen's University Belfast Research Portal

Mechanistic rationale to target PTEN-deficient tumour cells with inhibitors of the DNA damage response kinase ATM

Nuala McCabe [1,2*], Conor Hanna [1*] Steven M. Walker [1,2], David Gonda [3], Jie Li [3], Katarina Wikstrom [2], Kienan I. Savage [1], Karl T. Butterworth [1], Clark Chen [3], D. Paul Harkin [1,2], Kevin M. Prise [1] and Richard D. Kennedy [1,2].

[1]Centre for Cancer Research and Cell Biology, Queens University Belfast, Northern Ireland, BT9 7BL, [2]Almac Diagnostics, 19 Seagoe Industrial Estate, Craigavon, Northern Ireland, BT63 5QD and [3]University of California, San Diego, 3855 Health Science Drive #0987, La Jolla, CA 92093-0987.

* These authors contributed equally.

Running title: PTEN-deficient tumour cells are dependent on ATM signalling.

Word count: 2497

Conflict of Interest

Nuala McCabe, Steven M. Walker, Katarina Wikstrom, D. Paul Harkin and Richard D. Kennedy are all employees of Almac Group.

Financial support

This work was supported by Invest NI (reference ST263) through the European Sustainable Competitiveness Programme 2007-2013, European Regional Development Fund (ERDF) and grants S10-08 from Prostate Cancer UK and CE013_2-004: FASTMAN Centre, Movember Prostate Cancer Centre of Excellence.

Keywords

PTEN, ATM, oxidative stress, therapeutic target, DNA damage.

Corresponding Authors:

Richard D. Kennedy PHD

CCRCB

97 Lisburn Road

Queens University Belfast

Belfast

Northern Ireland

BT9 7BL

Telephone: +44 (0) 28 9097 2760

Fax: +44 (0)28 9097 2776

Email: r.kennedy@qub.ac.uk

Kevin M Prise PHD

CCRCB

97 Lisburn Road

Queens University Belfast

Belfast

Northern Ireland

BT9 7BL

Telephone: +44 (0) 28 9097 2760

Fax: +44 (0)28 9097 2776

Email: k.prise@qub.ac.uk

Abstract

ATM is an important signalling molecule in the DNA damage response (DDR). ATM loss of function can produce a synthetic lethal phenotype in combination with tumour-associated mutations in FA/BRCA pathway components. In this study, we took an siRNA screening strategy to identify other tumour suppressors which when inhibited similarly sensitized cells to ATM inhibition. In this manner, we determined that PTEN and ATM were synthetically lethal when jointly inhibited. PTEN-deficient cells exhibited elevated levels of reactive oxygen species, increased endogenous DNA damage and constitutive ATM activation. ATM inhibition caused catastrophic DNA damage, mitotic cell cycle arrest and apoptosis specifically in PTEN-deficient cells in comparison to wild-type cells. Antioxidants abrogated the increase in DNA damage and ATM activation in PTEN-deficient cells, suggesting a requirement for oxidative DNA damage in the mechanism of cell death. Lastly, the ATM inhibitor KU-60019 was specifically toxic to PTEN mutant cancer cells in tumour xenografts and reversible by re-introduction of wild-type PTEN. Together our results offer a mechanistic rationale for clinical evaluation of ATM inhibitors in PTEN-deficient tumours.

Abbreviations: PTEN, phosphatase and tensin homolog deleted on chromosome 10; ATM, ataxia telangiectasia mutated; DSB, double strand break; ROS, reactive oxygen species.

Introduction

Ataxia telangiectasia mutated (ATM) is the primary kinase, which responds to DNA double strand breaks (DSB) (1). Therapeutic inhibition of ATM has been shown to sensitize cells to ionising radiation and DNA damaging chemotherapeutic agents (2,3) suggesting that it may have a role in combination therapy for cancer. Increasingly, however, it has been found that DNA damage response targeted therapies, for example PARP inhibitors, may also exhibit single agent activity in the context of loss of specific tumour suppressors such as BRCA1 or BRCA2 (4) ATM inhibitors have a potential role as single agents in the context of loss of components of the FA/BRCA pathway (5). An siRNA library screen identified synthetic lethality between loss of ATM function and loss of various components of the FA/BRCA pathway that have been reported in human cancers. Combined loss of ATM and the FA/BRCA pathway resulted in the accumulation of lethal DNA damage and cell death. In the current study we ask if loss of ATM could be synthetically lethal with other known human tumour suppressors, thereby indicating other single agent targets for ATM inhibitors. We use an siRNA library designed to individually target known human tumour suppressors to screen against an isogenic ATM wild-type and deficient cell line system in order to identify synthetic lethal interactions. We consequently identify synthetic lethality between PTEN and ATM and demonstrate a role for ATM in promoting the survival of PTEN-deficient cells through the signalling of oxidative DNA damage.

Materials and Methods

Cell lines

All cell lines were sourced from the American Tissue Culture Collection (ATCC). HCT116 cells lacking wild-type PTEN have been described previously and were licensed from Georgetown University (6). The PC3-PTEN inducible cell lines (7) and

ATM deficient human fibroblasts and reconstituted cells have previously been described (8) (Supplementary Information and Supplementary Fig 1a).

Cell cycle, Apoptosis and Mitotic chromosome analysis

Cells were fixed in 70% ethanol, incubated with RNase A and propidium iodide (PI) and analysed with a FACSCalibur (Becton Dickinson) using CellQuest Pro software. For phospho-histone H3 analysis, cells were incubated with anti-phospho-histone H3 antibody (Upstate Biotechnology). Apoptotic assays were performed using the luminescence Caspase-Glo® 3/7 assay from Promega. To assess chromosome damage, cells were treated with colcemid (0.05μg/ml) (KaryoMAX, GibcoBRL) for 4 hours.

Western blotting analysis

Cell pellets were lysed in 20 mM Tris (pH 8), 200 mM NaCl, 1 mM EDTA, 0.5% (v/v) NP-40, 10% (v/v) glycerol. For phospho-H2AX detection, histones were extracted overnight at 4^{o}C in 0.2N HCL from protein pellets. Lysates and histone extracts were electrophoresed on NuPage pre-cast gels (Invitrogen), and immunoblotted with anti – phospho-H2AX (Cell Signalling Technology); anti-PTEN (Santa Cruz); anti- phospho-ATM ser1981 (Cell Signalling Technology); anti- phospho-CHK2 thr68 (Cell Signalling Technology) and anti- phospho-AKT ser473 (Cell Signalling Technology). As loading controls, anti- β-Actin (Sigma); anti- Vinculin (Cell Signalling Technology) and anti-Tubulin (Abcam) were used. This was followed by incubation with anti IgG-HRP (Cell Signaling Technology) and chemiluminescent detection (ECL-PLUS; Amersham, UK).

Reactive Oxygen Species Detection

Cells were incubated with 5μM CM-H_2DCF-DA (Invitrogen) for 30 minutes followed by flow cytometry.

Colony formation assays

Cells were seeded at predetermined densities, 24 hours later treated with KU-55933 (Calbiochem), which was replenished every 3-4 days. Where appropriate, cells were transfected with gene specific targeting siRNAs (Qiagen) using Lipofectamine™ RNAiMAX (Invitrogen) and 48 hours later counted and seeded for colony formation assay. After 10 days, cells were washed with PBS, fixed in methanol, stained with crystal violet and colonies counted. The surviving fraction (SF) for a given dose/siRNA was calculated and dose-response curves plotted using GraphPad Prism™ 5 * p=<0.05 Students-t test.

siRNA screening

A customised siRNA library targeting 178 tumour suppressor genes or genes whose loss of function was associated with cancer (Supplementary Table 1) was developed using predesigned siRNA sequences (Qiagen). The library contained 3 independent siRNA sequences per gene and was provided in an arrayed format in 96 well plates. ATM deficient and ATM complemented cells were reverse transfected with the siRNA library (Qiagen) using Lipofectamine RNAiMax reagent (Life Technologies) (Supplementary Information).

Xenograft study

3 x 10^7 cells were implanted into male Fox Chase Severe Combined Immunodeficiency (SCID) mice (Charles River Laboratories, Oxford, UK). Administration of doxycycline was started when tumours reached 100mm^3 in volume

and was performed every 48 hours up to removal of the animal from the experiment. 48 hours after PTEN induction, animals were administered KU-60019 (100mg/kg) for 5 consecutive days and measured until they reached a target 400mm^3 volume. Measurements of tumour volume and body weight took place every 3 days using calipers (Supplementary Information).

Results

ATM is a potential drug target for PTEN-deficient cells

In order to identify potential synthetic lethality interactions with ATM loss we used a customised siRNA library targeting 178 tumour suppressor genes (Supplementary Table 1). The library was used to screen against ATM-deficient and ATM-complemented fibroblasts (Supplementary Fig. 1A) (8). This isogenic cell line was found to be preferable to therapeutic ATM inhibition for the purpose of initial screening as there was less likely to be non-specific off-target interactions with the siRNA targets or the ATP-dependent reagents used for viability read-out. Robust Z-scores were calculated for 3 independent siRNA per gene and an average value was then generated. The screen identified 9 genes that were synthetically lethal with loss of PTEN (Table 1). Each of these 9 genes demonstrated an average Robust Z-score ≤ -2 (Fig. 1A.). Consistent with previous data, we found that components of the FA/BRCA pathway were synthetically lethal with ATM loss. In addition, CDKN2C and p53, genes involved in the G1/S checkpoint were synthetically lethal with ATM deficiency, indicating that they may play a compensatory role in maintaining cellular viability in the absence of ATM-mediated cell cycle check-pointing. Interestingly, the tumour suppressor PTEN was also synthetically lethal with ATM. Similar to ATM, PTEN had been reported to have a direct role in the DNA damage response (9-11) and loss of its function represented a potentially important drug target, as inactivating mutations are associated with incurable cancers such as advanced prostate cancer and glioblastoma (12). We therefore took PTEN forward into secondary validation as a synthetic lethal candidate.

For validation of PTEN as a hit from the screen, we performed colony formation assays in the ATM isogenic cells. PTEN knock-down using 2 independent siRNAs, resulted in reduced survival of ATM deficient cells compared to ATM wild-type

corrected cells (fold difference of 48% and 40%) (Fig.1B). Next, we assessed the sensitivity of the HCT116 (6) and PC3 (7) isogenic cell line models (Supplementary Fig. 1.A-B) to loss of ATM function using either gene specific siRNA or the ATM inhibitor KU-55933 (2). Both the PTEN-deficient cell-lines demonstrated increased sensitivity to siRNA mediated knock-down of ATM (fold difference of 20% and 42%) (Fig. 1C) and increased sensitivity to the KU-55933 (fold change in IC_{50} of 16 and 8) compared to wild-type counterparts (Fig. 1D). PTEN null cells have constitutive activation of AKT. We therefore ensured that KU-55933 did not inhibit AKT, and the observed sensitivity in PTEN null cells was independent of AKT function (Supplementary Fig. 2).

To confirm that the observed ATM inhibitor sensitivity in PTEN-deficient cells was not model specific, we tested a panel of cell-lines representing PTEN wild-type and deficient states in prostate cancer, glioblastoma, breast cancer and normal cells. In each case the PTEN-deficient cell line demonstrated increased sensitivity to the ATM inhibitor KU-55933 compared to the PTEN wild-type cell line (Supplementary Fig. 1C), suggesting that this strategy may be of value as a treatment in more than one cancer type. In addition, advanced prostate cancers and glioblastomas are associated with PTEN loss (12) and are often treated with radiation hence ATM inhibitors may be particularly useful in these indications where they may have a dual role.

PTEN-deficient cells have elevated levels of ROS, DNA damage and activation of ATM

It has previously been reported that PTEN-deficient cells exhibit abnormal homologous recombination (HR) mediated DNA repair through loss of expression of RAD51 (9, 13). However this observation has not been consistent across cell line models (10-11) or in human tumour samples (14). Loss of RAD51 expression could

potentially have accounted for the synthetic lethal interaction between PTEN and ATM. However, we did not find any association between RAD51 expression or foci formation and PTEN expression in our isogenic cell line systems with or without DNA damage, suggesting that HR functions normally in both cell lines (Supplementary Fig. 3A and Supplementary Fig. 3B). Moreover, both PTEN wild-type and deficient cells were sensitive to depletion of RAD51 by siRNA, the sensitivity being more pronounced in the deficient cells (Supplementary Fig. 3C). This further supports an alternative mechanism to loss of HR in PTEN deficient cells underlying the synthetic lethality with ATM inhibition.

PTEN null mouse embryonic fibroblasts have been reported to exhibit increased oxidative DNA damage (15), we therefore asked if there were increased levels of oxidative damage in the PC3 and HCT116 isogenic models. We used a fluorescence-based assay to measure reactive oxygen species (ROS) and observed a shift in the fluorescence-intensity of 10±1% and 12±2% associated with PTEN-deficiency in HCT116 and PC3 isogenic cell line models respectively (Fig. 2A). In addition there was a greater induction of ROS in PTEN-deficient compared to wild-type cells in the presence of the KU-55933 with increases of 21±2% and 25±3% in HCT116 and PC3 respectively. This observation suggests that ATM inhibition may further enhance oxidative stress in PTEN null cells. Oxidative DNA lesions have been reported to result in DSBs with consequent induction of histone-H2AX phosphorylation (γ-H2AX), a marker of DSBs (16). Consistent with this, the PTEN-deficient cell lines demonstrated increased baseline levels of γ-H2AX (Fig. 2B and Supplementary Fig. 3D). In addition, Western blot analysis demonstrated constitutive phosphorylation of ATM (a marker of activation) and its substrate Chk2, in PTEN-deficient cells (Fig. 2B), consistent with an ATM-mediated response to DSBs.

To further investigate if the observed increase in γ-H2AX and ATM phosphorylation in PTEN-deficient cells was the result of increased oxidative damage, we pre-treated the PTEN-deficient cell line HCT116 KO22 with the antioxidants N-acetyl cysteine or beta-carotene. Following treatment with these agents, we observed reduced γ-H2AX expression and phospho-ATM indicating that oxidative DNA damage was the likely cause for the increase in DSBs (Fig. 2C). In summary these data suggest that PTEN-deficient cells have high levels of oxidative stress, resulting in increased DNA damage and subsequent ATM activation.

Next we asked if the observed increase in oxidative DNA damage in PTEN-deficient cells was required for ATM inhibitor sensitivity. We pre-treated the HCT116 PTEN-deficient and wild-type isogenic cell lines with N-acetyl cysteine or beta-carotene and tested the sensitivity to the ATM inhibitor KU-55933 (Fig. 2D). Each of the antioxidants rescued KU-55933 sensitivity in the PTEN-deficient cell line, indicating that oxidative damage is required to sensitise PTEN-deficient cells to ATM inhibition.

Acute inhibition of ATM in PTEN-deficient cells results in cell cycle arrest, chromosome aberrations and apoptosis

To investigate how DNA damage following ATM inhibition resulted in a loss of cellular viability specifically in PTEN-deficient cells, we analysed the cell cycle profile of the cells with or without KU-55933 treatment. ATM inhibition resulted in a greater G2/M arrest in the HCT116 PTEN-deficient cells compared to wild-type cells (Fig. 3A). Furthermore, analysis of Histone H3 serine 10 phosphorylation (a measure of the mitotic cellular population) demonstrated that these cells were specifically arrested in mitosis (Fig. 3B). We then examined whether the accumulation of cells in M phase was associated with DNA damage. Chromosome spreads demonstrated an increase in aberrations, predominantly in the PTEN deficient cells, including radial

chromosomes following ATM inhibition, (Fig. 3C). This indicates that in PTEN-deficient cells, ATM normally functions to prevent catastrophic DNA damage progressing into the M phase of the cell cycle. Furthermore, treatment with the ATM inhibitor resulted in increased caspase 3/7 activation specifically in the HCT116 PTEN-deficient cell line (62%) compared to wild-type counterpart (8%) consistent with apoptotic cell death (Fig. 3D).

In vivo efficacy of ATM inhibition in PTEN-deficient xenografts

To investigate the *in vivo* efficacy of ATM specific inhibition in PTEN-deficient cells, we used the PC3 PTEN Tetracycline inducible cell line model in a subcutaneous xenograft setting. Firstly, we established that the Tetracycline derivative Doxycycline was efficient at inducing PTEN expression *in vitro* (Supplementary Fig. 4A) and *in vivo* (Supplementary Fig. 4B). Calliper measurements of tumour volumes showed that induction of PTEN using Doxycycline, led to a slowing of tumour growth from 72 hours onwards (Supplementary Fig. 4C). Next, we investigated the selective toxicity of the ATM specific kinase inhibitor KU-60019 (17) as a single modality in the PC3-PTEN inducible model. This inhibitor was chosen, as it is a potent ATM inhibitor and unlike KU-55933 is active in animal systems. Despite PTEN$^-$deficient control tumours reaching a 4-fold increase in size before PTEN wild-type controls, KU-60019 treated PTEN-deficient tumours displayed a statistically significant slowing in growth (Fig. 4A). This growth inhibition was especially evident at the start of the experiment (days 5-12) just after KU-60019 was administered (day 1-5). There were no significant changes in the mean relative body weights of each treatment groups (Fig. 4B). Inducible PTEN expression *in vivo* was analysed in resected tumours by immunofluorescence (Supplementary Fig. 4D).

Discussion

PTEN lost in a wide variety of human cancers (12), and its primary role as a tumour suppressor is through inhibition of the PI3/AKT pathway (18). However more recently, PTEN has been reported to maintain genomic integrity and confer resistance to ionising radiation and PARP inhibition (9-11,13), which is a nuclear function and independent from AKT regulation (19). In the current study we have reported a synthetic lethal interaction between loss of ATM and loss of PTEN. Loss of PTEN results in increased oxidative damage, which is required for the sensitization to ATM inhibition, as anti-oxidants can rescue PTEN-deficient cells from ATM-inhibitor-mediated cell death. Oxidative DNA lesions can result in stalled DNA replication forks and resultant DSBs (16) and activation of ATM (1). Hence loss of ATM function in PTEN-deficient cells may therefore result in a persistence of oxidative DNA lesions and inactivation of the G2M checkpoint, allowing cells with catastrophic DNA damage to enter the M phase of the cell cycle and undergo cell death. Importantly, ATM has been reported to function to prevent malignant progression of pre-malignant conditions through the signalling of oncogene-related DNA damage (20). Our data suggest that once a cell has become malignant through additional genetic abnormalities e.g. loss of PTEN, the cancer cell can then become dependent on ATM activation to maintain a level of DNA integrity required for survival. In summary, we have demonstrated that PTEN and ATM are synthetically lethal, and furthermore we have found a requirement for ATM in the maintenance of DNA integrity and cellular viability in the presence of increased oxidative damage secondary to PTEN deficiency. The selective sensitivity of PTEN-deficient tumours to ATM inhibition *in vivo* suggests that this may represent a novel approach to targeted cancer therapy in the clinic.

Acknowledgments

We thank Professor T Waldman for the HCT116 PTEN isogenic cell line model.

References

1. Shiloh Y, Ziv Y. The ATM protein kinase: regulating the cellular response to genotoxic stress, and more. Nat Rev Mol Cell Biol 2013;14:197-210.
2. Hickson I, Zhao Y, Richardson CJ, Green SJ, Martin NM, Orr AI, et al. Identification and characterization of a novel and specific inhibitor of the ataxia-telangiectasia mutated kinase ATM. Cancer Res 2004;64:9152-59.
3. Batey MA, Zhao Y, Kyle S, Richardson C, Slade A, Martin NM, et al. Preclinical evaluation of a novel ATM inhibitor, KU59403, in vitro and in vivo in p53 functional and dysfunctional models of human cancer. Mol Cancer Ther 2013;12:959-67.
4. Lord CJ, Ashworth A. Targeted therapy for cancer using PARP inhibitors. Curr Opin Pharmacol 2008;8:363-9.
5. Kennedy RD, Chen CC, Stuckert P, Archila EM, De la Vega MA, Moreau LA, et al. Fanconi anemia pathway-deficient tumor cells are hypersensitive to inhibition of ataxia telangiectasia mutated. J Clin Invest 2007;117:1440-9.
6. Lee C, Kim JS, Waldman T. PTEN gene targeting reveals a radiation-induced size checkpoint in human cancer cells. Cancer Res 2004;64:6906-14.
7. Maxwell PJ, Coulter J, Walker SM, McKechnie M, Neisen J, McCabe N, et al. Potentiation of inflammatory CXCL8 signaling sustains cell survival in *PTEN*-deficient prostate carcinoma. Eur Urol 2013;64:177-88.
8. Ziv Y, Bar-Shira A, Pecker I, Russell P, Jorgensen TJ, Tsarfati I, et al. Recombinant ATM protein complements the cellular A-T phenotype. Oncogene 1997;15:159-67.
9. Shen WH, Balajee AS, Wang J, Wu H, Eng C, Pandolfi PP, et al. Essential role for nuclear PTEN in maintaining chromosomal integrity. Cell 2007;128:157-70.
10. Gupta A, Yang Q, Pandita RK, Hunt CR, Xiang T, Misri S, et al. Cell cycle checkpoint defects contribute to genomic instability in PTEN-deficient cells independent of DNA DSB repair. Cell Cycle 2009;8:2198-210.
11. McEllin B, Camacho CV, Mukherjee B, Hahm B, Tomimatsu N, Bachoo RM, et al. PTEN loss compromises homologous recombination repair in astrocytes: implications for glioblastoma therapy with temozolomide or poly(ADP-ribose) polymerase inhibitors. Cancer Res 2010;70:5457-64.
12. Li J, Yen C, Liaw D, Podsypanina K, Bose S, Wang SI, et al. PTEN, a putative protein tyrosine phosphatase gene mutated in human brain, breast, and prostate cancer. Science 1997;275:1943-47.
13. Mendes-Pereira AM, Martin SA, Brough R, McCarthy A, Taylor JR, Kim JS, et al. Synthetic lethal targeting of PTEN mutant cells with PARP inhibitors. EMBO Mol Med 2009;1:315-22.
14. Fraser M, Zhao H, Luoto KR, Lundin C, Coackley CL, Chan N, et al. PTEN Deletion in Prostate Cancer Cells Does Not Associate With Loss of RAD51 Function: Implications for Radiotherapy and Chemotherapy. Clinical Cancer Research 2012;18:1025-27.
15. Huo YY, Li G, Duan RF, Gou Q, Fu CL, Hu YC, Song BQ, et al. PTEN deletion leads to deregulation of antioxidants and increased oxidative damage in mouse embryonic fibroblasts. Free Radic Biol Med 2008;44:1578-91.
16. Harper JV, Anderson JA, O'Neill P. Radiation induced DNA DSBs: Contribution from stalled replication forks? DNA Repair 2010;9:907-13.
17. Golding SE, Rosenberg E, Valerie N, Hussaini I, Frigerio M, Cockcroft XF, et al. Improved ATM kinase inhibitor KU-60019 radiosensitizes glioma cells, compromises insulin, AKT and ERK prosurvival signaling, and inhibits migration and invasion. Mol Cancer Ther 2009;8:2894-902.
18. Manning BD, Cantley LC. AKT/PKB signaling: navigating downstream. Cell 2007;129:1261-74.

19. Bassi C, Ho J, Srikumar T, Dowling RJ, Gorrini C, Miller SJ, et al. Nuclear PTEN controls DNA repair and sensitivity to genotoxic stress. Science 2013;341:395-9.
20. Bartkova J, Rezaei N, Liontos M, Karakaidos P, Kletsas D, Issaeva N, et al. Oncogene-induced senescence is part of the tumorigenesis barrier imposed by DNA damage checkpoints. Nature 2006;444:633-7.

Figure Legends

Figure 1: ATM is a potential drug target for PTEN-deficient cells

A. Robust Z score distribution of siRNAs targeting 178 tumour suppressor genes in ATM isogenic cell line models.

B. Colony formation assay demonstrating synthetic lethality in the ATM fibroblast isogenic model system, transfected with 2 independent siRNAs specifically targeting PTEN (Qiagen). Survival fractions were calculated based on scrambled control, transfected cells. (* p = <0.05 Students-t test). (Validation of the siRNA targeting PTEN, Supplementary Fig. 1B).

C. Colony formation assay demonstrating synthetic lethality in the HCT116 and PC3 PTEN isogenic model systems, transfected with 2 siRNAs specifically targeting ATM (Qiagen) (Validation of the siRNA targeting ATM, Supplementary Fig. 1B) (* p = <0.05 Students-t test). PTEN wild-type cells: HCT WT and PC3+PTEN and PTEN deficient cells, HCT KO22 and PC3-PTEN.

D. Colony formation assay demonstrating synthetic lethality in the HCT116 and PC3 PTEN isogenic model systems, treated with increasing concentrations of the ATM inhibitor KU-55933. Survival fractions were calculated based on DMSO treated cells. Solid lines indicate PTEN wild-type cells and broken lines indicate PTEN-deficient cells.

Figure 2: PTEN-deficient cells have elevated levels of ROS, DNA damage and activation of ATM

A. Oxidative stress assay demonstrating increased basal reactive oxygen species in (i) HCT116 (ii) PC3 PTEN isogenic cells. ** p= <0.01 and *** p= <0.001 Students-t test.

B. Increase d γ-H2AX, phospho-ATM serine 1981 and phospho-CHK2 threonine 68 levels in PTEN HCT116 (KO22) and PC3 (PC3-PTEN) deficient cells compared to wild-type counter-parts. Total ATM and CHK2 were used as loading controls.

C. Reversal of increased γ-H2AX and phospho-ATM levels in PTEN-deficient HCT116 and PC3 cells treated with 100μM β-carotene or 10μM NAC. β-Actin and total ATM were used as loading controls.

D. Colony formation assay of PTEN wild-type and deficient HCT116 cells treated with 10μM KU-55933 in the absence and presence of 100μM β-carotene or 10μM NAC. * p= <0.05 Students-t test.

Figure 3: Acute inhibition of ATM in PTEN null cells results in cell cycle arrest, chromosome aberrations and apoptosis

A. G2/M arrest in PTEN-deficient HCT116 cells treated with 10μM KU-55933 for 72 hours (* p = <0.05).

B. M phase arrest in PTEN-deficient HCT116 cells treated with 10μM KU-55933 for 72 hours (* p = <0.05). % increase from DMSO treated cells.

C. Increased chromosome breaks and aberrations in PTEN-deficient HCT116 cells after treatment with 10μM KU-55933 for 72 hours (* p = <0.05).

D. HCT116 wild-type and KO22 cells were treated with 10μM KU-55933 for 96 hours and analysed for caspase 3/7 activation (* p = <0.05). % increase from DMSO treated cells.

Figure 4: *In vivo* efficacy of ATM inhibition in PTEN-deficient xenografts

A. Relative tumour volume curves for $PTEN^{+/+}$ untreated control (●), $PTEN^{-/-}$ untreated control (●), KU-60019 treated $PTEN^{+/+}$ (■) and $PTEN^{-/-}$ (■) PC-3 xenografts. Mean relative tumour volume is plotted against time from initial treatment. Target tumour volume was $400mm^3$ i.e. 4-fold increase in size from initial treatment. T-tests were performed at 30 days. Each treatment group contained 4 animals.

B. Box plot of mean relative change in body weight during treatments.

Gene	Function	Average Z Score
BRIP1 (FANCJ)	DNA repair	-10.029
CDKN2C	G1/S checkpoint	-8.373
PTEN	Negative regulator PI3K	-6.256
STEAP4	Immunity and response to oxidative stress	-5.322
NKTR	Immunity	-4.452
CASP8	Apoptosis	-2.541
TP53	G1/S checkpoint	-2.459
FANCG	DNA repair	-2.316
CAV1	Cell cycle progression/RAS signalling	-2.023

Table 1. siRNA hits

Figure 1: ATM is a potential drug target for PTEN deficient cells

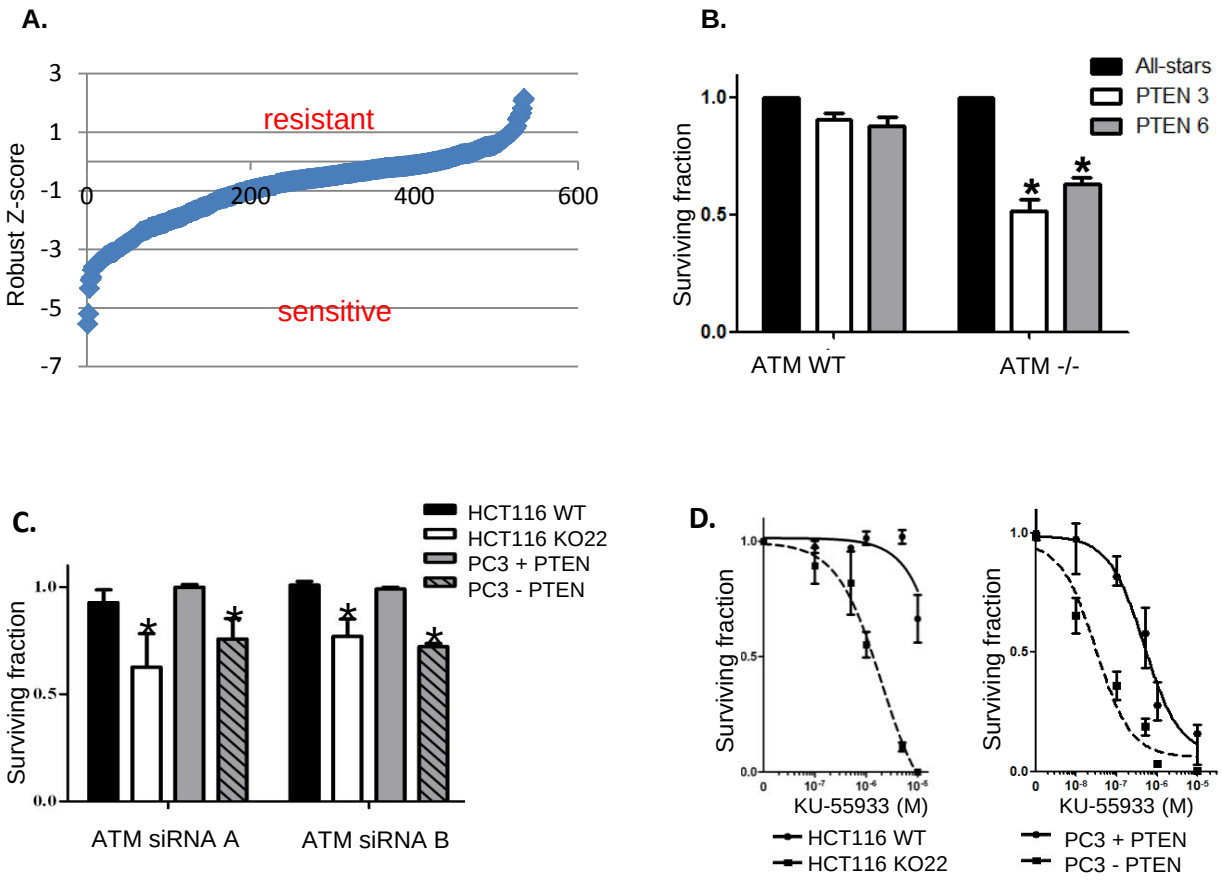

Figure 2. PTEN null cells have elevated levels of ROS, DNA damage and activated ATM kinase which is rescued by treatment with anti-oxidants

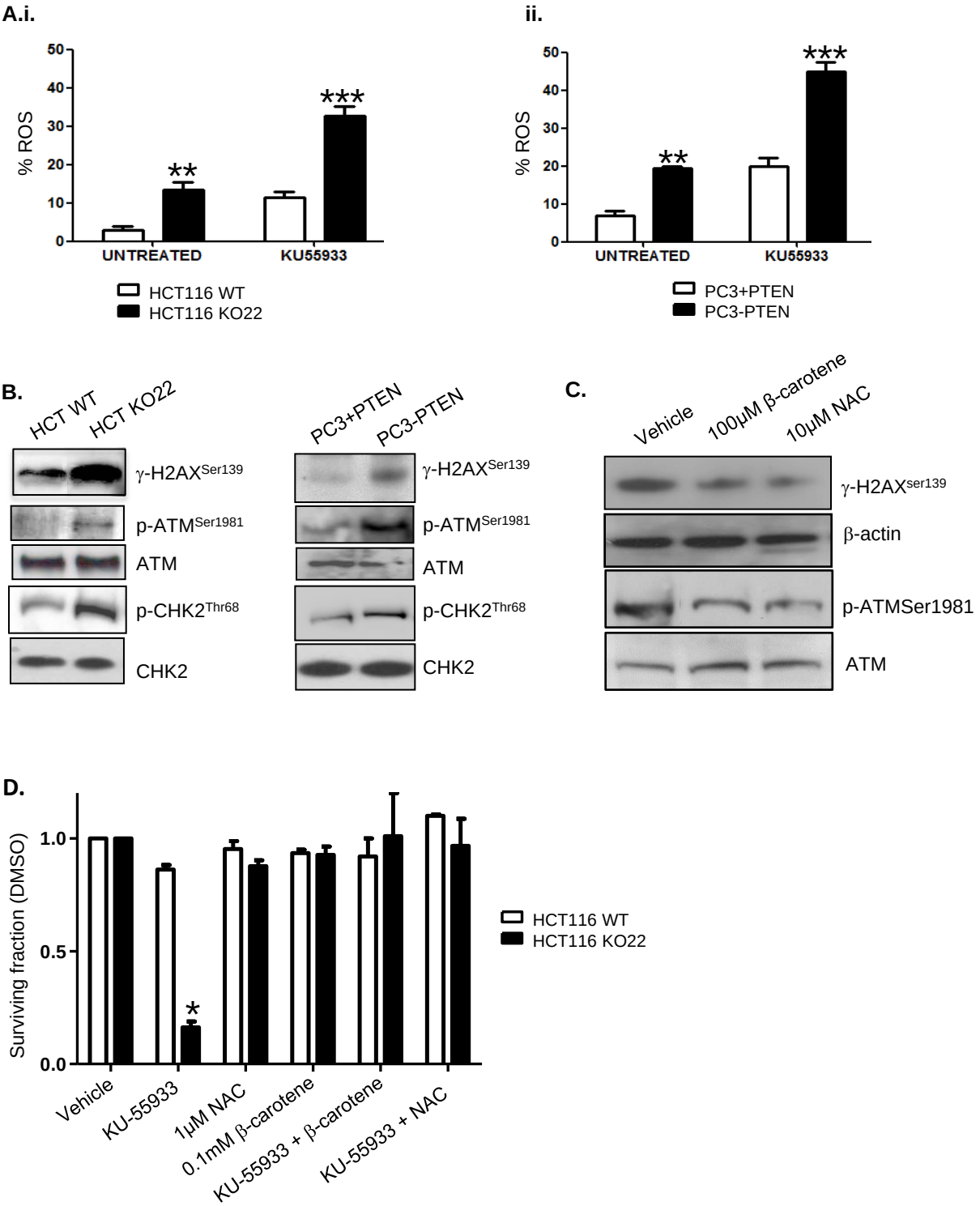

Figure 3. Acute inhibition of ATM in PTEN null cells results in cell cycle arrest, chromosome aberrations and apoptosis

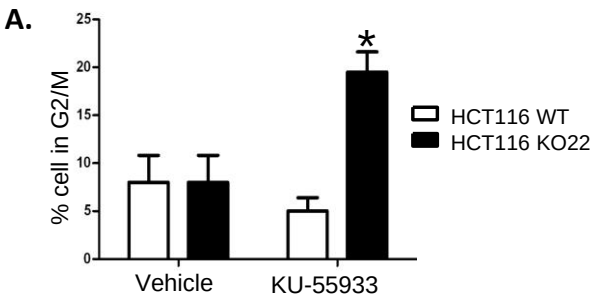

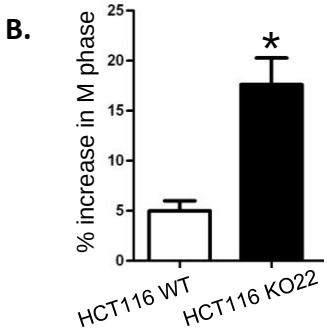

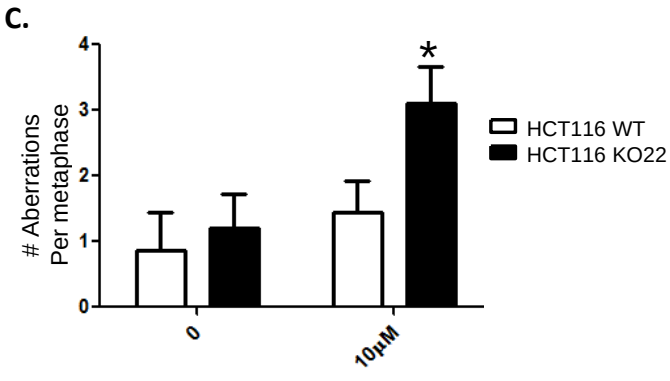

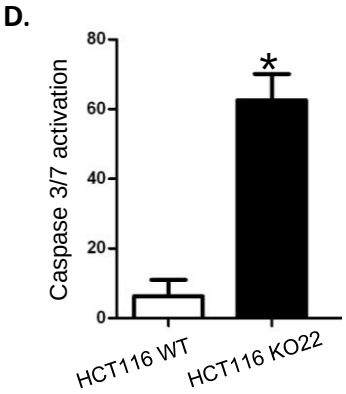

Figure 4. *In vivo* efficacy of ATM inhibition with PTEN loss

A.

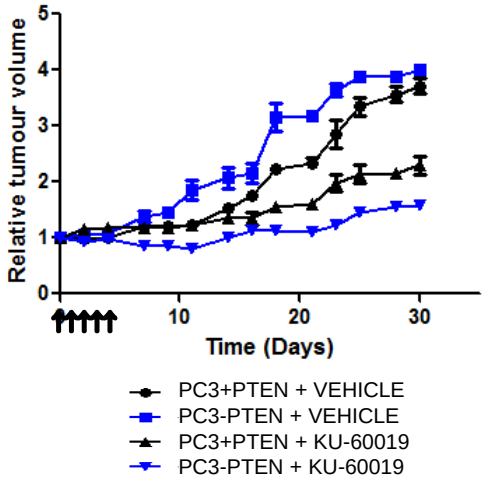

B.

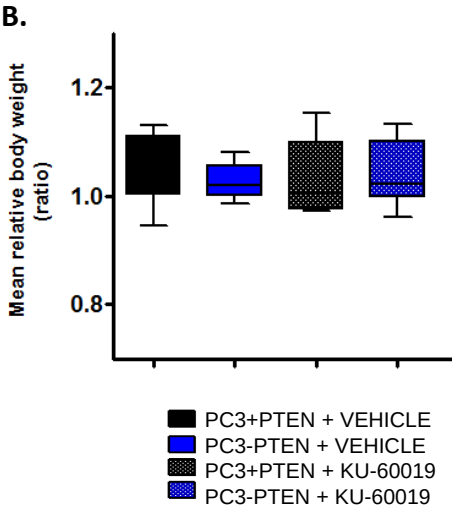

COMPARISON	T-Test
PTEN WT VS DEFICIENT (VEHICLE)	0.3218
PTEN WT VEHICLE VS PTEN WT KU60019	0.1213
PTEN DEFICIENT VEHICLE VS KU60019	0.0004
PTEN WT VS PTEN DEFICIENT (KU60019)	0.006

Supplementary Information

Supplementary Figure legends

Figure 1: ATM is a potential drug target for PTEN-deficient cells

A.i. Stable expression of recombinant FLAG tagged-ATM or empty vector in the ATM deficient fibroblast cell line AT22IJE-T, and correlation with phosphorylation of CHK2 on threonine 68 in the absence/presence of 6 Gy IR as indicated. Total CHK2 and gamma-tubulin were used as loading controls.

ii. Epression of PTEN in the HCT116 cell line model in wild-type cells and loss of expression in a knock-out clone (KO22). The inverse correlation of pAKT serine 473 is also shown.

iii. Inducible expression of wild-type PTEN in the PC3 prostate cancer cell line after 72H tetracycline addition. The inverse correlation of pAKT serine 473 is also shown.

B.i. Knockdown of PTEN using 2 independent siRNAs. Untransfected and Scrambled transfected cells were used as controls. Beta-tubulin was used as a loading control.

ii. Knockdown of ATM using 2 independent siRNAs. Untransfected and Scrambled transfected cells were used as controls. Vinculin was used as a loading control.

C.i. Western blot analysis of PTEN expression in a panel of cancer and normal cell lines.

ii. Colony formation assay showing sensitivity to the ATM inhibitor KU-55933 in a panel of cancer and normal cell lines.

Figure 2: The synthetic lethality with PTEN loss and ATM inhibition is independent of AKT function

A. Phospho-AKT serine473 expression in PTEN deficient KO22 cells treated with (i) 1 and 10μM KU-55933 and (ii) 1, 5 and 10μM MK2206 (AKT inhibitor) for 48 hours.

B. Colony formation assay of PTEN wild-type and deficient HCT116 cells treated with 5μM MK2206 and 10μM KU-55933 and then in combination. Survival fraction was normalized to DMSO.

Figure 3: The synthetic lethality with PTEN loss and ATM inhibition is independent of RAD51 function

A. RAD51 expression in the PTEN isogenic cell lines (i) and across a panel of PTEN-deficient and wild-type cell lines (ii).

B. Increased RAD51 focus formation in HCT116 PTEN wild-type cells with and without HU treatment. Data is representative of 3 independent experiments. * p=<0.05 Students-t test.

C. (i) Colony formation assay of PTEN wild-type and deficient HCT116 and PC3 cells transfected with RAD51 siRNA. Survival fraction was normalized to scrambled control. (ii) Western blotting analysis of the RAD51 siRNA was performed in the HCT116 wild-type cells using 10nM siRNA and beta-actin as a loading control.

D. Increased gamma-H2AX foci formation in HCT116 PTEN-deficient cells. Positive cells were counted as cells with more than five foci in three independent experiments.

Supplementary Figure 4: *In vivo* efficacy of ATM inhibition with PTEN loss

A. Western blot analysis of PTEN-inducible PC-3 tumour cells exposed to 2μg/ml of doxycycline or tetracycline *in vitro*.

B. Western blot analysis of PTEN-inducible PC-3 subcutaneous tumours resected from SCID mice at specific time points (0-28 days) following initial oral gavage administration of doxycycline [16mg/kg].

C. Tumour volumes (mm^3) were measured to assess the effect doxycycline-induction of tumour suppressor PTEN had on tumour growth (●) (vs. control (■)). Each experimental condition consisted of 4 mice. Error bars represent ± standard error of the mean (SEM).

D. Co-staining of resected xenograft tumours by immunofluorescence for DAPI (Blue) and PTEN (Green).

Materials and Methods

Cell lines

All cell lines were sourced from the American Tissue Culture Collection (ATCC). HCT116 cells lacking wild-type PTEN have been described previously and were licensed from Georgetown University (1). PTEN exon II was deleted from these cells by homolgous recombination using the cre-lox system resulting in complete loss of the PTEN protein in the KO22 cells (Supplementary Fig. 1a). The PC3-PTEN inducible cell lines were generated using the Virapower T-Rex™ Lentiviral Expression System (Invitrogen) which resulted in Tetracycline-inducible expression of full-length PTEN in the PTEN mutant PC3 cell line (Supplementary Fig. 1a) (2). ATM deficient and complemented cells have previously been described (3). AT22IJE-T, was derived from primary A-T fibroblasts and harbor a homozygous frameshift mutation at codon 762 of the ATM gene resulting in an unstable truncated protein. These cells were complemented with either the ATM full-length gene or an empty vector (Supplementary Fig. 1a) (3). All cell lines were validated by STR profiling.

siRNA screening

ATM isogenic cells were reverse transfected with the siRNA library (Qiagen) using Lipofectamine RNAiMax reagent as per manufacturer's instructions (Life

Technologies) 2000 cells were transfected with 10nM siRNA. 24 hours later media was changed into normal growth media. 48 hours post-transfection cells were split at a ratio of 1:3 into new 96 well plates. The cells were allowed to grow for 10 days until ~80% confluent. Cell viability was assayed using the Cell titre Glo assay (Promega). The sensitivity of the screen was monitored by (i) PLK1 siRNA causing a reduction in viability of more than 90% in both cell types, when compared to transfection with a non-targeting siRNA control (All-stars) (ii) Z-factor (4) for the cell lines was >0.5 (for ATM wild-type 0.543 and ATM deficient 0.580). The siRNA screen was performed once and the average robust z-scores of the 3 independent siRNAs targeting each gene was determined for each cell line.

γH2AX focus formation

Cells were fixed in 4% paraformaldehyde and permeablised with 0.5% Triton X-100/ PBS and stained with mouse monoclonal anti- γH2AX (Ser-139), 1:200 (20E3; Cell Signaling, UK). Positive cells were counted as cells with more than five foci in three independent experiments.

***In vivo* study**

Subcutaneous xenograft tumours derived from the PC-3 PTEN tetracycline-inducible cell model were grown in male Fox Chase SCID (Severe Combined Immunodeficiency) mice (Charles River Laboratories, Oxford, UK.). PC-3 Cells were suspended fresh autoclaved PBS at 3 x 10^7 cells per ml and kept on ice until implantation. Implantation required mice to be anaesthetised. 100 µl of cell suspension (3 x 10^6 cells) was injected subcutaneously into the right flank of each mouse using a sterile syringe and 21G needle. Simultaneously, mice were

subcutaneously implanted with transponders for unique identification (Avid Identification Systems, California, USA).

For *in vivo* studies, KU-60019 was dissolved in Hot Rod Chemistry (HRC) Rapid Formulation 6 (Pharmatek Laboratories, California, USA) to improve solubility and bioavailability. When tumour volumes reached 100 mm^3, mice were randomly assigned into treatment groups. KU-60019 [100 mg/kg] and drug vehicle were administered orally once daily, for 5 consecutive days. PTEN was induced in the specified $PTEN^{+/+}$ tumours by the oral gavage administration of 100 µl doxycycline [16 mg/kg] and repeated every 48 hours up to 14 days post-initial treatment. All experiments were carried out in accordance with the local ethical and Home Office Regulations (ASPA19/ project licence 2945) and designed in accordance with the Scientific Procedures Act (1986) and the 2010 Guidelines for the welfare and use of animals in cancer research (5).

Measurement of Tumour Volumes

4 animals were used per treatment group. This was calculated for effects which differ by 20%, with a standard deviation of 10% and results in an 80% power to detect the effect with statistical significance ($p < 0.05$, two-tailed t-test) (6). Xenograft tumour generation was monitored from 1 week following injection onwards using volumetric measurements with external callipers. Measurements of tumour volume and body weight took place every 3 days. In order to assess tumour volume by external callipers, the greatest longitudinal diameter (length), the greatest transverse diameter (width) and the greatest vertical diameter (breadth) were measured and the geometric mean diameter (GMD) calculated. Tumour volume estimates could then be derived.

$$GMD = \sqrt[3]{(L \times B \times H)}$$

$$r = \frac{GMD}{2}$$

$$volume = \left(\frac{4}{3}\right) \times (\pi \times r^3)$$

1. Lee, C., Kim, J.S., and Waldman, T. PTEN gene targeting reveals a radiation-induced size checkpoint in human cancer cells. Cancer Res. 2004; 64: 6906-6914.
2. Maxwell, PJ., Coulter, J., Walker, SM., McKechnie M., Neisen J., McCabe, N. et al. Potentiation of inflammatory CXCL8 signaling sustains cell survival in *PTEN*-deficient prostate carcinoma. Eur Urol. 2013 Aug;64(2):177-88.
3. Ziv Y, Bar-Shira A, Pecker I, Russell P, Jorgensen TJ, Tsarfati I, Shiloh Y. Recombinant ATM protein complements the cellular A-T phenotype. Oncogene. 1997 Jul 10;15(2):159-67.
4. Zhang JH, Chung TD, Oldenburg KR. A Simple Statistical Parameter for Use in Evaluation and Validation of High Throughput Screening Assays. J Biomol Screen. 1999;4(2):67-73.
5. Workman P, Aboagye EO, Balkwill F, Balmain A, Bruder G, Chaplin DJ, et al. Guidelines for the welfare and use of animals in cancer research. Br J Cancer. 2010 May 25;102(11):1555-77.
6. Suresh KP and Chandrashekara S. Sample size estimation and power analysis for clinical research studies. J Hum Reprod Sci. 2012 Jan-Apr; 5(1): 7–13.

Supplementary Table 1: siRNA target genes (tumour suppressor genes or genes whose loss has been implicated in cancer development)

Entrez Gene Id	NCBI gene symbol
324	APC
613	BCR
857	CAV1
1031	CDKN2C
1869	E2F1
2297	FOXD1
3055	HCK
4163	MCC
4763	NF1
5728	PTEN
472	ATM
641	BLM
858	CAV2
1033	CDKN3
1958	EGR1
2313	FLI1

3090	HIC1
4221	MEN1
4771	NF2
5888	RAD51
545	ATR
672	BRCA1
999	CDH1
1111	CHEK1
2067	ERCC1
2353	FOS
3091	HIF1A
4255	MGMT
4820	NKTR
5925	RB1
580	BARD1
675	BRCA2
1026	CDKN1A
1540	CYLD
2177	FANCD2
2355	FOSL2
3726	JUNB
4292	MLH1
4978	OPCML
5931	RBBP7
581	BAX
694	BTG1
1027	CDKN1B
1612	DAPK1
2189	FANCG
2547	XRCC6
3727	JUND
4436	MSH2
5157	PDGFRL
5933	RBL1
595	CCND1
754	PTTG1IP
1028	CDKN1C
1630	DCC
2195	FAT1
2873	GPS1
3732	CD82
4481	MSR1
5245	PHB
5934	RBL2
596	BCL2
836	CASP3
1029	CDKN2A
1647	GADD45A
2196	FAT2
2874	GPS2

3814	KISS1
4616	GADD45B
5591	PRKDC
6041	RNASEL
602	BCL3
841	CASP8
1030	CDKN2B
1755	DMBT1
2241	FER
2956	MSH6
4089	SMAD4
4681	NBL1
5727	PTCH1
6251	RSU1
6400	SEL1L
7048	TGFBR2
7411	VBP1
8061	FOSL1
8797	TNFRSF10A
9821	RB1CC1
10744	PTTG2
11319	ECD
26524	LATS2
51684	SUFU
6648	SOD2
7157	TP53
7428	VHL
8314	BAP1
8844	KSR1
9940	DLEC1
10912	GADD45G
11334	TUSC2
27156	RTDR1
51741	WWOX
6764	ST5
7158	TP53BP1
7490	WT1
8438	RAD54L
9113	LATS1
10078	TSSC4
11068	CYB561D2
21933	Tnfrsf10b
28316	CDH20
51752	ERAP1
6767	ST13
7159	TP53BP2
7507	XPA
8535	CBX4
9232	PTTG1
10168	ZNF197

11144	DMC1
22908	SACM1L
28513	CDH19
54879	ST7L
6768	ST14
7161	TP73
7520	XRCC5
8555	CDC14B
9537	TP53I11
10256	CNKSR1
11145	PLA2G16
23221	RHOBTB2
29997	GLTSCR2
54979	HRASLS2
6794	STK11
7184	HSP90B1
7873	ARMET
8556	CDC14A
9540	TP53I3
10263	CDK2AP2
11178	LZTS1
25855	BRMS1
29998	GLTSCR1
55294	FBXW7
6868	ADAM17
7251	TSG101
7982	ST7
8626	TP63
9589	WTAP
10395	DLC1
11186	RASSF1
25900	IFFO1
51213	LUZP4
57110	HRASLS
6886	TAL1
7260	TSSC1
7991	TUSC3
8743	TNFSF10
9705	ST18
10641	TUSC4
11200	CHEK2
26255	PTTG3
51352	WIT1
57509	MTUS1
57786	RBAK
84445	LZTS2
286827	TRIM59
64061	TSPYL2
84955	NUDCD1
338440	ANO9

79577	CDC73
94241	TP53INP1
79689	STEAP4
120114	FAT3
79728	PALB2
124641	OVCA2
83937	RASSF4
129025	ZNF280A
83990	BRIP1
140883	ZNF280B
84312	BRMS1L
283455	KSR2

Supplementary data

Supp Figure 1. Validation of PTEN cell line models and synthetic lethality across tumour types

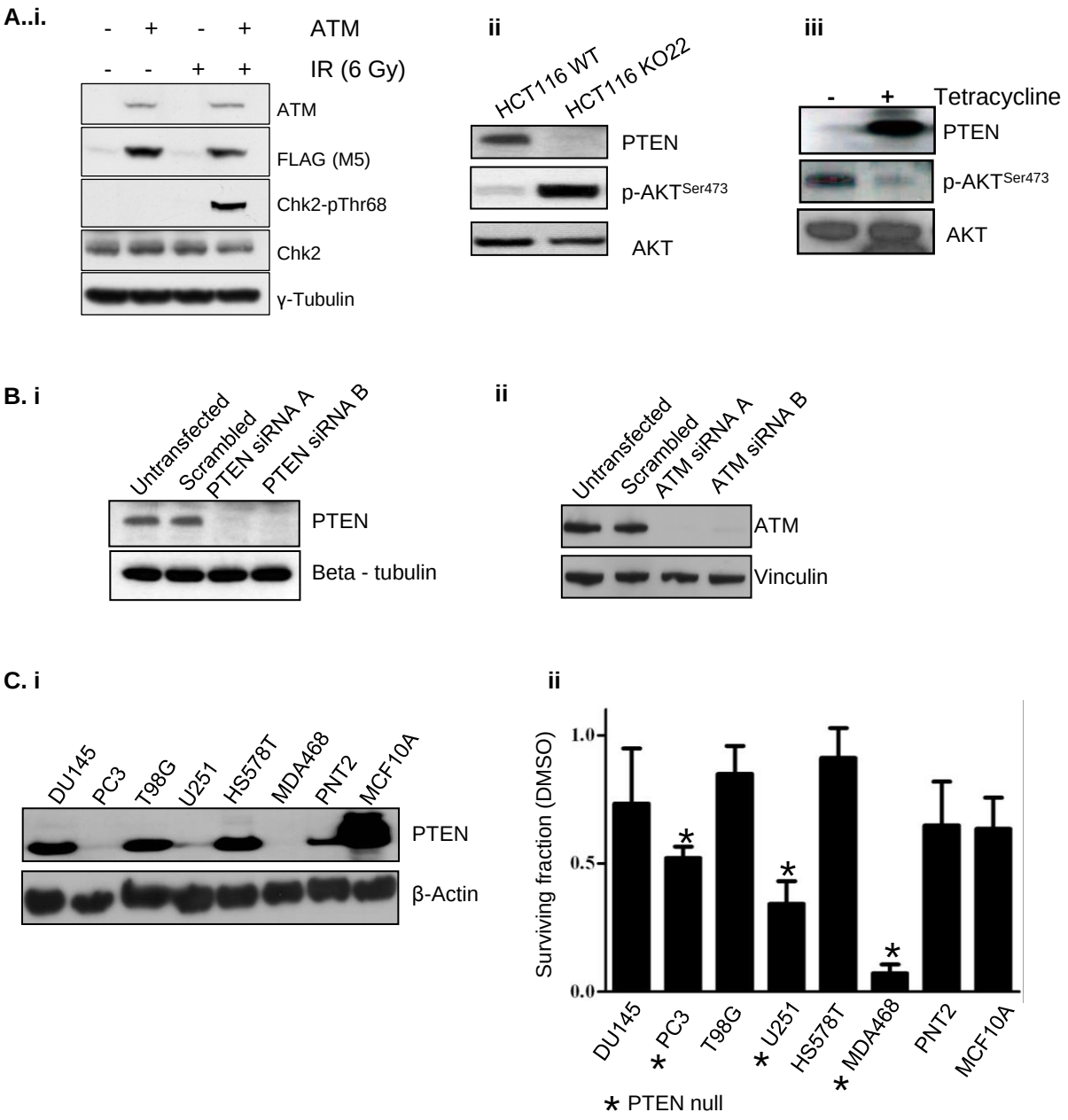

Supp Figure 2. The synthetic lethality with PTEN loss and ATM inhibition is independent of AKT function

A.i.

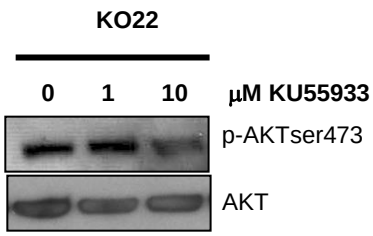

ii.

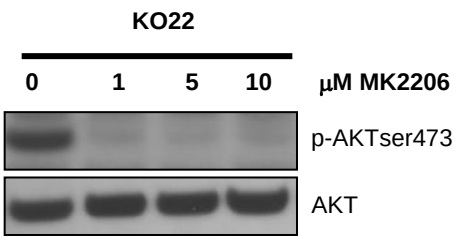

B.

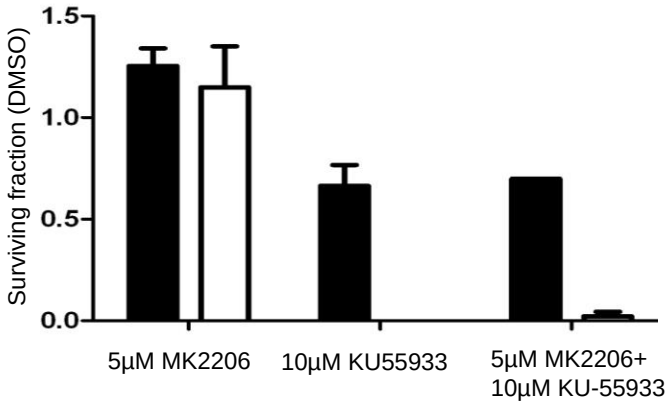

Supp Figure 3. The synthetic lethality with PTEN loss and ATM inhibition is independent of RAD51 function

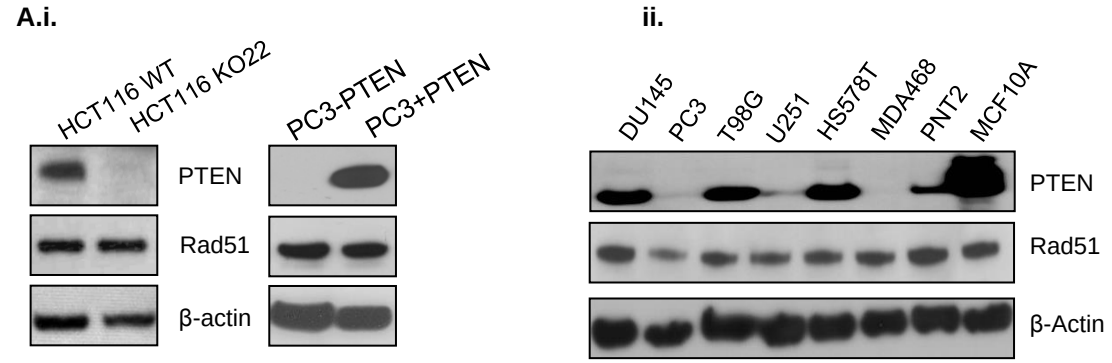

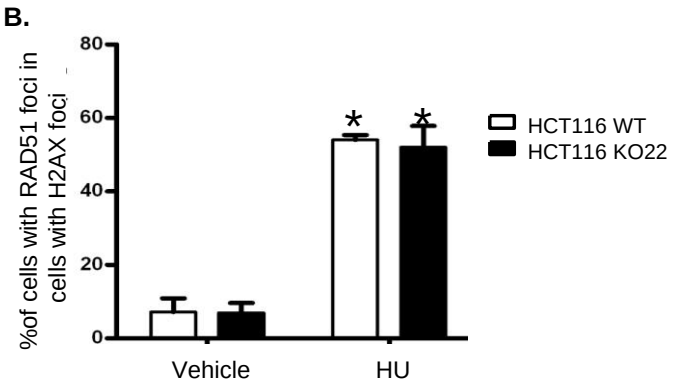

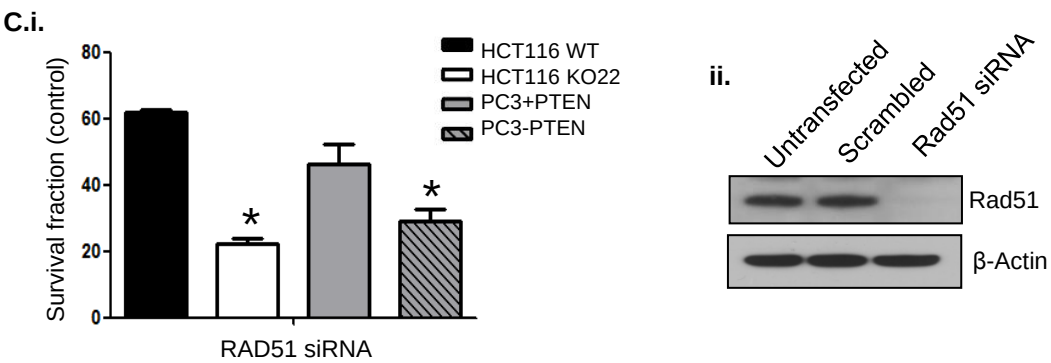

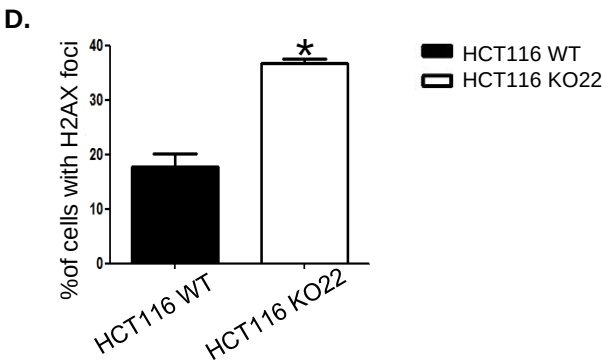

Supplementary Figure 4: *In vivo* efficacy of ATM inhibition in PTEN deficient xenografts